Biochimica et Biophysica Acta 1852 (2015) 2432–2441

Contents lists available at ScienceDirect

Biochimica et Biophysica Acta

journal homepage: www.elsevier.com/locate/bbadis

Fatostatin, an SREBP inhibitor, prevented RANKL-induced bone loss by suppression of osteoclast differentiation

Kazuki Inoue [a], Yuuki Imai [a,b,*]

[a] Division of Laboratory Animal Research, Advanced Research Support Center, Ehime University, Ehime, Japan
[b] Division of Integrative Pathophysiology, Proteo-Science Center, Graduate School of Medicine, Ehime University, Ehime, Japan

ARTICLE INFO

Article history:
Received 8 May 2015
Received in revised form 31 July 2015
Accepted 24 August 2015
Available online 28 August 2015

Keywords:
Osteoclast
Fatostatin
DNase-seq
Srebf2
Micro CT

ABSTRACT

Osteoclast differentiation is associated with both normal bone homeostasis and pathological bone diseases such as osteoporosis. Several transcription factors can regulate osteoclast differentiation, including c-fos and Nfatc1. Using genome-wide DNase-seq analysis, we found a novel transcription factor, SREBP2, that participates in osteoclast differentiation *in vitro*. Here, we asked whether SREBP2 actually plays a role in controlling bone metabolism *in vivo*. To answer this question, RAW264 cells, primary cultured osteoclasts and the mouse RANKL-induced bone loss model were treated with fatostatin, a small molecule inhibitor specific for the activation of SREBP. When cells were treated with fatostatin, osteoclast differentiation was impaired. Similar results were obtained following treatment with siRNA for *Srebf2*, the gene coding for SREBP2. *In vivo*, μCT analyses showed that fatostatin treatment preserved bone mass and structure in the proximal tibial trabecular bone in the mouse RANKL-induced bone loss model. In addition, bone histomorphometric analysis revealed that the protection of bone mass by fatostatin might have been achieved by suppression of RANKL-mediated osteoclast differentiation. These results indicated that the novel transcription factor SREBP2 physiologically functions in osteoclast differentiation *in vivo* and might be a possible therapeutic target for bone diseases.

1. Introduction

Bone tissue is continuously remodeled by osteoclastic bone resorption and osteoblastic bone formation [1]. Together, osteoclasts and osteoblasts maintain bone homeostasis [2]. Abnormal osteoclast differentiation or activity causes an imbalance in bone remodeling and results in skeletal diseases, including osteoporosis and osteopetrosis [3]. Osteoclast differentiation consists of multiple steps. Preosteoclasts differentiate from monocyte/macrophage lineage cells after stimulation by macrophage colony-stimulating factor (M-CSF) and receptor activator of NF-κB ligand (RANKL). Subsequently, preosteoclasts fuse and differentiate into mature multinucleated osteoclasts [4]. This differentiation process must be tightly regulated by a complex network of various osteoclastogenic transcription factors, such as c-Fos [5], and nuclear factor of activated T cells calcineurin-dependent 1 (Nfatc1) [6]. These transcription factors successively and cooperatively induce the expression of osteoclastogenic genes including tartrate-resistant acid phosphatase (*Acp5*) [7] and Cathepsin K (CtsK) [8]. Therefore, elucidation of the transcriptional mechanism underlying osteoclast differentiation is essential for understanding both the physiology of bone homeostasis and the pathology of skeletal disorders.

To unravel the transcriptional mechanism underlying osteoclast differentiation, we previously performed DNase-seq [9], which is a powerful tool to identify DNase hypersensitive sites (DHSs) and transcription factors binding to the DHSs [10]. We used a RANKL-dependent differentiation model with the murine macrophage cell line, RAW264. In the study, we succeeded in identifying osteoclast-specific DHSs. This genome-wide information allowed us to identify not only well-known transcription factors but also novel transcription factors in osteoclast differentiation, such as Atf1, Zscan10, Nrf1 and Srebf2. These novel transcription factors positively regulate osteoclast differentiation *in vitro*. However, their precise physiological and pathological functions in bone metabolism are still unknown. To investigate the functions of these transcription factors, we have initially focused on SREBP2 (encoded by *Srebf2*). SREBP2 is a master regulator of cholesterol metabolism [11], and several studies found a strong relationship between osteoclast differentiation/function and cholesterol homeostasis [12–14].

Sterol regulatory element binding protein 2 (SREBP2) is best known as a transcription factor regulating cholesterol homeostasis through transcriptional activation of its target genes, including LDL receptor, HMG-CoA synthase and HMG-CoA reductase [15,16]. SREBP2 has a basic-helix-loop-helix leucine zipper (bHLH-Zip) domain at the N-terminal side and its regulatory domain is at the C-terminal side [17].

Abbreviations: SREBP, sterol regulatory element binding protein; RANKL, receptor activator of nuclear factor kappa B ligand; M-CSF, macrophage colony-stimulating factor; TRAP, tartrate-resistant acid phosphatase; CtsK, Cathepsin K; LdlR, low-density lipoprotein receptor.

* Corresponding author at: Shitsukawa, Toon, Ehime 791-0295, Japan.
E-mail address: y-imai@m.ehime-u.ac.jp (Y. Imai).

http://dx.doi.org/10.1016/j.bbadis.2015.08.018
0925-4439/

After synthesis as a full-length protein, SREBP2 is bound to the endoplasmic reticulum (ER) membrane where it forms a complex with SREBP cleavage activating protein (SCAP) [18]. When intracellular cholesterol levels are reduced, SREBP2 is proteolytically cleaved by S1P and S2P proteases at the membrane to release the N-terminal amino acids containing the bHLH-Zip domain, generating the mature form of SREBP2 [19,20]. Mature SREBP2 translocates into the nucleus and binds to sterol regulatory elements (SREs) within the promoter region of its target genes to activate their transcription [21]. SREBP2 is ubiquitously expressed, and the physiological functions of SREBP2 in cholesterol metabolism have been explored in several tissues, including hepatocytes, adipocytes, endothelial cells, macrophages and male germ cells [22–25].

SREBP2 functions *in vivo* have been investigated by the utilization of tissue-specific SREBP2-overexpressing transgenic (SREBP2-Tg) mice. PEPCK promoter-driven SREBP2-Tg mice conditionally overexpress SREBP2 in the liver and adipose tissue, and analysis of the Tg mice revealed that SREBP2 preferentially activates cholesterol biosynthesis rather than fatty acid synthesis in the liver and adipose tissue [22]. Pancreatic β-cell specific SREBP2-Tg mice under control of the rat insulin promoter exhibited severe diabetes due to loss of β-cell mass with accumulation of cholesterol [26]. Intestinal SREBP2-Tg mice showed an increase of cholesterol levels not only in the jejunum but also in the serum [27]. Although SREBP2-Tg mice revealed physiological roles of SREBP2, phenotypes of Tg mice do not always reflect physiological conditions. Therefore, loss-of-function studies *in vivo* are required to investigate the true physiological functions of SREBP2. However, systemic SREBP2 knockout mice show complete embryonic lethality at an early stage of development [28,29], and conditional SREBP2 knockout mice have not yet been reported. Recently, to analyze the loss of SREBP (SREBP1a, 1c and 2) functions *in vivo*, a small molecule compound that inhibits activation of SREBPs has been discovered. The inhibitor, named fatostatin, blocks SREBP translocation from the ER to the Golgi apparatus through binding to SCAP [30]. Long-term fatostatin treatment reduced body weight, blood glucose levels and adiposity in *ob*/*ob* mice through its inhibition of SREBP activation. We therefore postulated that the physiological functions of SREBP2 in osteoclasts might be elucidated by inhibition of SREBP2 activation by fatostatin treatment. To test this hypothesis, we investigated whether fatostatin treatment affected SREBP2 activation in osteoclasts, osteoclast differentiation *in vitro* and bone metabolism *in vivo* using a RANKL-induced bone loss model.

2. Materials and methods

2.1. Animals and cell lines

C57BL/6J female mice were purchased from CLEA Japan. Animal experiments were approved by the Animal Experiment Committee of Ehime University and were performed in accordance with the Guidelines of Animal Experiments of Ehime University. Murine RAW264 cells and MC3T3-E1 cells were obtained from the RIKEN cell bank (RIKEN BRC, Japan). RAW264 cells were cultured in osteoclast culture medium (Minimum Essential Media Alpha (MEM α) (Life Technologies, USA) supplemented with 10% Cellect fetal bovine serum (FBS) (MP Biomedicals, USA), 1% antibiotic–antimycotic solution (Life Technologies) and 1% MEM non-essential amino acids (Life Technologies)). MC3T3-E1 cells were maintained in osteoblast culture medium (MEM α supplemented with 10% FBS (Nichirei Biosciences, Inc., Japan), and 1% antibiotic–antimycotic solution).

2.2. Primary osteoclast differentiation

Primary osteoclast differentiation was performed as previously described [9]. Briefly, murine bone marrow macrophages (BMMs) were isolated from the humeri, femora and tibiae of C57BL6 female mice at 8 weeks of age and were maintained in osteoclast culture medium with 10 ng/mL M-CSF for 2 days. For osteoclast differentiation, BMMs were plated in 6-well plates at a density of 1×10^5 cells/well and were treated with 234 ng/mL GST-RANKL (Oriental Yeast Co., Ltd., Japan) and 10 ng/mL M-CSF (R&D Systems, USA) for 3 days. At each indicated time point, cells were collected for RNA extraction.

2.3. siRNA transfection of RAW264 cells and osteoclast differentiation

siRNA transfection and osteoclast differentiation assay were performed as previously described [9]. Briefly, AllStar negative control siRNA (Qiagen, USA) and *Srebf2* siRNA (Sigma-Aldrich, USA) were used at a final concentration of 150 nM. Each siRNA was transfected into RAW264 cells (1×10^5 cells) using the Neon transfection system (Invitrogen). Following transfection (36 h) total RNAs were extracted from transfected cells and subjected to real-time RT-PCR. For osteoclast differentiation, RAW264 cells were seeded in 24-well plates at a density of 1×10^4 cells/well and were treated with 117 ng/mL GST-RANKL for 3 days. Differentiated cells were fixed with 4% paraformaldehyde (PFA) for 15 min. After washing with phosphate-buffered saline (PBS) twice, the fixed cells were permeabilized with an equal volume mixture of acetone and ethanol for 30 s and then treated with TRAP staining solution (0.01% naphthol AS-MX phosphate (Sigma-Aldrich) and 0.06% Fast Red Violet LB Salt (Sigma-Aldrich) in 50 mM sodium tartrate dehydrate and 45 mM sodium acetate (pH 5.0)). TRAP-positive multinucleated cells (>3 nuclei/cell) were counted as mature osteoclasts.

2.4. Cell viability assay

Cell viability assays were performed by using an MTT (3-(4,5-dimethyl-2-thiazolyl)-2,5-diphenyltetrazolium bromide) Cell Count Kit (Nacalai Tesque, Japan) according to the manufacturer's protocol. RAW264 cells and BMMS were seeded in 96-well plates at a density of 1.25×10^4 cells/well. The cells were treated with vehicle (EtOH) or fatostatin (5, 10, 15, 20 μM) for 48 h. Then, 10 μL of MTT solution (5 mg/mL) was added in each well, and the cells were incubated for 3 h in the CO_2 incubator. After incubation, the media were aspirated and cells were dissolved by addition of 100 μL of solubilization solution. Then, the absorbance at 570 nm (reference: 650 nm) was measured with a FlexStation 3 (Molecular Devices, Japan).

2.5. Osteoblast differentiation

In vitro osteoblast differentiation was performed by using MC3T3-E1 cells. MC3T3-E1 cells were plated in 6-well plates and were cultured with osteoblast culture medium until they became fully confluent. Then, medium was replaced with osteoblast differentiation medium (osteoblast culture medium supplemented with 100 ng/mL BMP-2 (R&D, USA), 50 μg/mL ascorbic acid, and 10 mM β-glycerophosphate). Cells were collected at each indicated time point for RNA extraction.

2.6. Real-time RT-PCR (RT-qPCR)

RNA extraction and real-time RT-PCR were performed as previously described [9]. Briefly, total RNA was extracted with Sepasol-RNA I Super G (Nacalai Tesque, Japan) and an RNeasy Mini Kit (Qiagen, USA) according to the manufacturers' instructions. Total RNA was reverse transcribed with a PrimeScript RT Master Mix (Takara Bio, Inc., Japan) according to the manufacturer's instructions. Real-time PCR was performed with Kapa SYBR Fast qPCR Kits (Kapa Biosystems, USA) and the Thermal Cycler Dice Real-Time System (Takara Bio, Inc., Japan). The *Rplp0* gene served as an internal control. Specific primers for each gene are listed below:

Rplp0: 5′-TTCCAGGCTTTGGGCATCA-3′ and 5′-ATGTTCAGCATGTTCAGCAGTGTG-3′; *Srebf1*: 5′-TGGTTGTTGATGAGCTGGAG-3′ and 5′-GGCTCTGGAACAGACACTG-3; *Srebf2*: 5′-TGCACCAGAGAGCATTTT

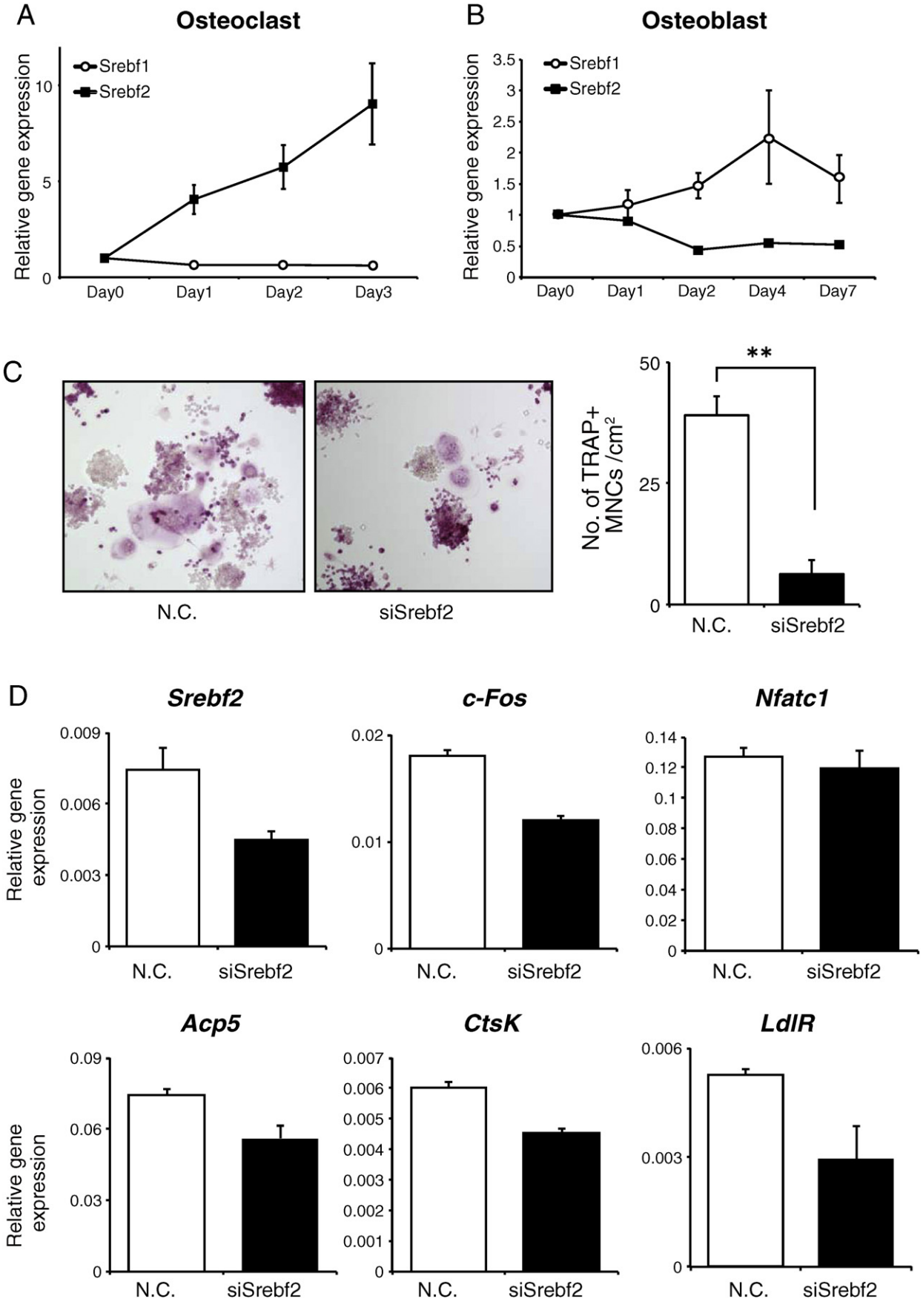
A
Osteoclast
Relative gene expression
Srebf1
Srebf2
Day0
Day1
Day2
Day3
B
Osteoblast
Relative gene expression
Srebf1
Srebf2
Day0
Day1
Day2
Day4
Day7
C
N.C.
siSrebf2
No. of TRAP+ MNCs /cm²
**
N.C.
siSrebf2
D
Srebf2
c-Fos
Nfatc1
Relative gene expression
N.C.
siSrebf2
Acp5
CtsK
LdlR
Relative gene expression
N.C.
siSrebf2

GC-3′ and 5′-AGGAACAAAGATGCCACAG-3′; c-*Fos*: ATGTTCTCGGGT TTCAACGC-3′ and 5′-CGCAAAAGTCCTGTGTGTTG-3′; *Nfatc1*: 5′-GGGACCAACCGTATTTCCACAC-3′ and 5′-TCGGTAGCCAGCCAGGAA TC-3′; *Acp5*: 5′-TTGCGACCATTGTTAGCCACATA-3′ and 5′-TCAGAT CCATAGTGAAACCGCAAG-3′; *Ctsk*: 5′-ACCACTTGGGAGACATGACC-3′ and 5′-ACCAACACTGCATGGTTCA-3′; *LdlR*: 5′-AATGGGGGCAAT CGGAAAAC-3′ and 5′-TGGCACTGAAAATGGCTTCG-3′.

2.7. Western blotting

RAW264 cells were treated with ethanol (EtOH) or fatostatin (10 μM, Merck Millipore, USA) for 24 h. Cells were washed with ice-cold PBS and dissolved with RIPA buffer (50 mM Tris–HCl, pH 8.0, 150 mM NaCl, 1% Nonidet P-40, 0.5% sodium deoxycholate, 0.1% SDS, 1 mM EDTA and protease inhibitors). Whole-cell extracts were separated by SDS-PAGE and transferred to polyvinylidene fluoride (PVDF) membranes. The membranes were blocked with 5% skim milk in PBS with Tween-20 (PBST). Then, anti-Srebp2 antibody (4 μg/mL, ab30682, Abcam, USA), anti-Srebp1 antibody (2 μg/mL, ab3259, Abcam, USA) or anti-β-actin antibody (1 μg/mL, 2F3, Wako, Japan) was bound overnight at 4 °C. After washing with PBST, HRP-conjugated secondary antibody (1:1500, Dako) was bound for 1 h at room temperature. Immunoreactive signals were detected with Chemi-Lumi One Ultra (Nacalai Tesque, Japan) and ImageQuant LAS 4000 (GE Healthcare, USA).

2.8. RANKL-induced bone loss model, fatostatin treatment and serum biochemistry

RANKL-induced bone loss was established as previously reported [31,32]. Briefly, GST-RANKL (2 mg/kg) or PBS was injected intraperitoneally into 7-week-old female mice. After 48 h, the mice were sacrificed and the tibias were harvested for μCT and histological analysis. To investigate the effect of fatostatin on this bone loss model, fatostatin (30 mg/kg, Merck Millipore, USA) was injected intraperitoneally 48 h before the first RANKL injection. Fatostatin injections were conducted at 24-h intervals for 4 days before sacrifice. Five mice were used in each group.

To examine the long-term effects of fatostatin, vehicle or fatostatin (30 mg/kg) was injected intraperitoneally into 7-week-old female mice twice a week for 3 weeks. After long-term treatment with fatostatin, the mice were sacrificed, and the sera were collected for measurement of serum lipids and the tibias were harvested for μCT analysis. Seven mice were used in each group. Serum lipids (total cholesterol, triglycerides, HDL and LDL) were measured at a commercial laboratory (Oriental Yeast Co., Ltd., Japan).

2.9. Micro-computed tomography (μCT) analysis

Micro-computed tomography (μCT) analysis was performed as previously reported [33,34]. Tibias were fixed with 70% ethanol and subjected to μCT analysis using a Scanco Medical μCT35 System (Scanco Medical, Switzerland) with an isotropic voxel size of 6 μm for trabecular analyses according to the manufacturer's instructions and the guidelines of the American Society for Bone and Mineral Research (ASBMR) [35]. Two hundred slices of proximal tibial metaphysis starting at 0.6 mm from the end of the growth plate were scanned and analyzed. Three-dimensional reconstructions were generated and analyzed according to the manufacturer's instructions and the ASBMR guidelines [35].

2.10. Bone histomorphometry

For TRAP staining, tibias were fixed in 70% ethanol for 3 days, and the nondecalcified bones were embedded in methyl methacrylate. Longitudinal 5-μm thick sections were cut on a microtome (Leica RM2255, Leica Microsystems, Germany) and subjected to TRAP staining using a TRAP/ALP Stain kit (Wako, Japan) according to the manufacturer's protocol. Histomorphometry of the secondary spongiosa was performed with the OsteoMeasure analysis system (OsteoMetrics, USA) at 200-fold magnification according to the ASBMR guidelines [36].

2.11. Statistical analysis

Statistical analyses were performed as previously described [9] with Excel (Microsoft, USA) or SPSS (IBM, USA). Data were evaluated by a two-tailed Student's t-test or by one-way analysis of variance (ANOVA) followed by Bonferroni post hoc tests. For all graphs, data are shown as means ± standard deviation (SD). Statistical significance is indicated as *, $p < 0.05$ and **, $p < 0.01$.

3. Results

3.1. Srebf2 positively regulated osteoclast differentiation in vitro

To clarify the functions of the *Srebf2* gene in osteoclasts, we first analyzed changes of *Srebf2* mRNA expression during primary osteoclast differentiation. *Srebf2* mRNA was remarkably increasing during osteoclast differentiation, whereas the expression level of *Srebf1* mRNA was not changed (Fig. 1A), suggesting that *Srebf2* but not *Srebf1* might have a major role in osteoclast differentiation. To the contrary, *Srebf1* mRNA increased and *Srebf2* mRNA decreased during osteoblast differentiation (Fig. 1B). These results indicated that *Srebf2* might predominantly regulate osteoclast differentiation. We then investigated the functions of *Srebf2* in osteoclast differentiation using gene silencing. Knockdown of *Srebf2* using siRNA led to a significant decrease in the number of TRAP-positive multinucleated osteoclasts compared with the control siRNA transfected cells (Fig. 1C). Gene expression analysis showed that gene silencing of *Srebf2* decreased the expression of osteoclast differentiation marker genes, including *Fos*, *Acp5* and *Ctsk* as well as *LdlR*, which is a target gene of SREBP2 (Fig. 1D). These results suggested that *Srebf2* might be a positive regulator of osteoclast differentiation.

3.2. Fatostatin inhibited osteoclast differentiation in vitro

To reveal the physiological functions of *Srebf2*/SREBP2 in osteoclast differentiation, we sought to analyze bone metabolism in SREBP2 knockout mice. However, systemic SREBP2 knockout mice showed embryonic lethality [28], and SREBP2 floxed mice have not been available. Therefore, we tried to abrogate the functions of SREBP2 through the *in vivo* use of an inhibitor of SREBP2 activation. Fatostatin is a recently described small organic molecule that inhibits the activation of SREBPs. Fatostatin treatment was shown to improve hyperglycemia and excessive accumulation of fat in the livers of *ob*/*ob* mice [30]. Hence, we hypothesized that fatostatin would impair osteoclast differentiation by blocking of the activation of SREBP2.

Fig. 1. *Srebf2* positively regulated osteoclast differentiation *in vitro*. Relative mRNA expression levels of *Srebf1* and *Srebf2* during A) osteoclast and B) osteoblast differentiation were measured by RT-qPCR (n = 3 biological replicates). Bars represent means ± SD. C) The two left panels show representative images of TRAP staining of RAW264 cells transfected with negative control siRNA (N.C.) or si*Srebf2*. The number of TRAP-positive multinucleated cells (TRAP+ MNCs) was counted (n = 4 biological replicates). Bars represent means ± SD. **, $p < 0.01$ versus N.C. D) RAW264 cells were transfected with siRNA for either N.C. or *Srebf2* for 36 h. RT-qPCR (n = 3 biological replicates) was used to assess relative mRNA expression levels of *Srebf2*, *Fos*, *Nfatc1*, *Acp5*, *CtsK* and *LdlR*. Bars represent means ± SD.

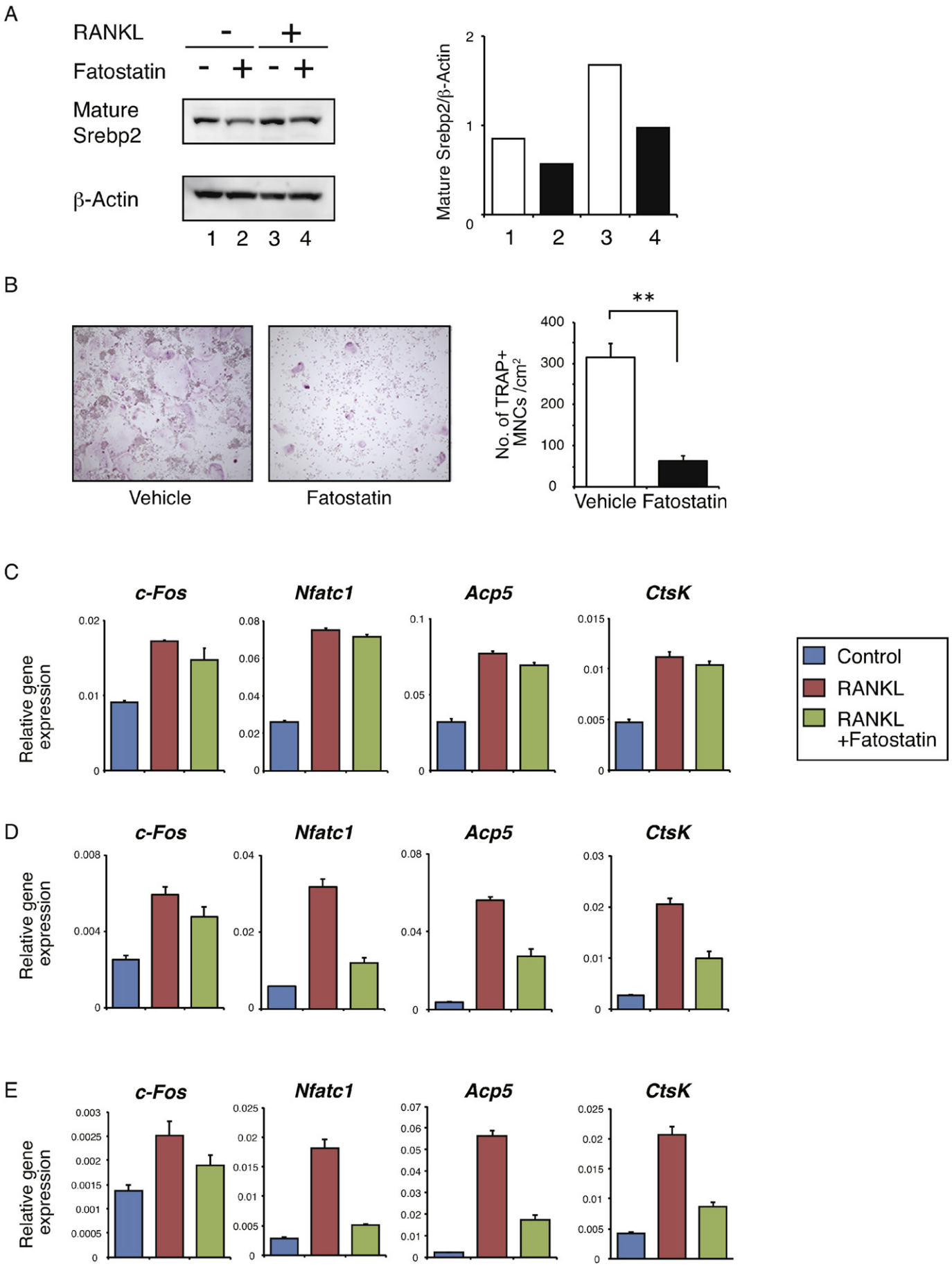
A
RANKL
Fatostatin
Mature Srebp2
β-Actin
1 2 3 4
Mature Srebp2/β-Actin
B
Vehicle
Fatostatin
No. of TRAP+ MNCs /cm²
Vehicle Fatostatin
C
c-Fos
Nfatc1
Acp5
CtsK
Relative gene expression
Control
RANKL
RANKL +Fatostatin
D
E

First, we examined whether fatostatin inhibited the activation of SREBP2 in osteoclasts. RAW264 cells were treated with fatostatin for 24 h, and the levels of mature SREBP2 protein were assessed by Western blotting. We observed that mature SREBP2 protein was decreased by fatostatin treatment (Fig. 2A, lane 2) compared with vehicle treatment (lane 1). In addition, it was increased by RANKL stimulation (lane 3) and RANKL-induced SREBP2 maturation was abrogated by fatostatin treatment (lane 4), suggesting that fatostatin blocked the cleavage and the activation of SREBP2 in osteoclasts. Meanwhile, mature SREBP1 protein was decreased by fatostatin treatment (Fig. S1, lane 2) compared with vehicle treatment (lane 1). In addition, RANKL treatment decreased mature SREBP1 protein levels (lane 3), and RANKL-induced SREBP1 maturation was unchanged by fatostatin (lane 4), suggesting that fatostatin inhibited the cleavage of SREBP1 in macrophage-like cells, while fatostatin did not affect the cleavage of SREBP1 in the presence of RANKL. Next, we investigated the effects of fatostatin on osteoclast differentiation. As fatostatin has cytotoxic effects on RAW264 cells and BMMs at high concentration (15–20 μM), we examined the effects of fatostatin on osteoclast differentiation at 10 μM (Fig. S2). Treatment of RAW264 cells with fatostatin remarkably suppressed RANKL-induced osteoclast differentiation and significantly decreased the number of TRAP-positive multinucleated osteoclasts compared with vehicle treated cells (Fig. 2B). To investigate the effects of fatostatin on osteoclastic gene expression, mRNA expression analyses during osteoclast differentiation were performed. Consistent with a previous report [37], osteoclast marker genes were upregulated by RANKL for 24 h and they were gradually decreased until 72 h. The expression of marker genes upregulated by RANKL was not affected by fatostatin at the early stage of osteoclast differentiation (Fig. 2C), whereas fatostatin treatment significantly reduced osteoclast marker gene expression after 48 h (Fig. 2D and E). These data showed that fatostatin inhibited *in vitro* osteoclast differentiation by hampering the activation of SREBP2 and the subsequent transcriptional activation of osteoclastic genes.

3.3. Fatostatin suppressed bone loss and osteoclast differentiation in a RANKL-induced bone loss model

To supplement the *in vitro* observations above, we examined the *in vivo* pharmacological effects of fatostatin on bone metabolism. First, we investigated the effects of fatostatin on bone metabolism under physiological conditions. Vehicle or fatostatin was delivered intraperitoneally into 7-week-old female mice for 3 weeks. After long-term treatment with fatostatin, we evaluated its effects on cholesterol and bone metabolism. While the serum levels of HDL were slightly reduced in the fatostatin-treated mice, other serum lipids and the bone parameters in the fatostatin-treated mice were not changed compared to those in the control mice (Fig. S3). These results suggested that fatostatin might not affect bone and cholesterol metabolism under physiological conditions. Therefore, we next examined the effects of fatostatin on bone metabolism under pathological conditions. Towards that end, we administered fatostatin to mice using a RANKL-induced bone loss model. In this model, acute loss of trabecular bone is caused by increased osteoclastic bone resorption within two days without alteration of osteoblastic bone formation parameters [31]. Fatostatin, RANKL or vehicles were injected intraperitoneally according to the experimental schedule shown in Fig. 3A. Forty-eight hours after RANKL injection, the mice were sacrificed and the tibiae were harvested. To evaluate the effects of fatostatin on bone mass and its structure in RANKL-induced bone loss, we performed μCT analysis of the tibiae obtained from mice that were treated with or without RANKL and fatostatin. Representative 3D reconstructions of proximal tibial trabecular bone showed that RANKL-induced bone loss was prevented by fatostatin treatment (Fig. 3B). Analysis of the 3D parameters revealed that fatostatin treatment significantly rescued the RANKL-induced decrease of trabecular BV/TV and Tb. N, and increased Tb. Sp. (Fig. 3C), whereas fatostatin had no effect on cortical bone parameters that were not impaired by RANKL treatment (Fig. 3D). These results indicated that fatostatin might prevent RANKL-induced trabecular bone loss.

To reveal how fatostatin rescued RANKL-induced bone loss and whether fatostatin affected osteoclast differentiation *in vivo*, we performed bone histomorphometric analyses using TRAP staining of the sections of proximal tibial trabecular bones obtained from each group (Fig. 4A). Bone histomorphometric analyses showed that osteoclast surfaces and the number of TRAP-positive osteoclasts per bone perimeter were significantly increased by RANKL treatment, and the elevation of these osteoclastic parameters was completely blocked in fatostatin-treated mice (Fig. 4B). These results suggested that fatostatin might inhibit osteoclast differentiation *in vivo* and prevent bone loss induced by increased bone resorption, such as occurs in osteopenia.

4. Discussion

Transcriptional regulation of osteoclast differentiation involves several transcription factors [38]. To gain further insights into the transcriptional mechanisms underlying osteoclast differentiation, we previously performed DNase-seq to identify open chromatin regions during osteoclast differentiation and succeeded in identifying several novel transcription factors, including *Srebf2* [9]. However, the physiological functions of Srebf2/SREBP2 in osteoclasts have not been clear. In this study, we demonstrated that SREBP2 appeared to positively regulate osteoclast differentiation *in vivo* as well as *in vitro* by using an inhibitor of SREBPs, fatostatin.

SREBP2 is well known as a master regulator of cholesterol homeostasis with positive transcriptional regulation of LDLR and HMG-CoA reductase [28]. Recent studies reported that exogenous cholesterol is important for osteoclast differentiation and survival. The absence of exogenous cholesterol, including LDL, impaired osteoclast formation, fusion, morphology and survival [13]. LDLR knockout mice showed increased bone mass with reduced osteoclast fusion and spreading [39]. Moreover, it has been reported that simvastatin, one of the cholesterol-lowering statins, inhibited osteoclast differentiation and reduced bone loss in a RANKL-induced bone loss model [32]. In our current study, we showed that SREBP2 knockdown in osteoclasts led to decreased expression of *Ldlr* mRNA. Therefore, one of the possible mechanisms through which SREBP2 controls osteoclast differentiation might be mediated through *Ldlr* gene expression and cholesterol uptake.

In this study, we showed that SREBP2 knockdown reduced not only *LdlR* mRNA but also *Fos* mRNA. Therefore, SREBP2 might transcriptionally control non-cholesterogenic genes to regulate osteoclast differentiation. SREBP2 knockdown decreased *Fos* mRNA levels. However, mRNA levels of *Nfatc1* (a target of *Fos*) were not changed (Fig. 1D). This result indicated that *Fos* mRNA levels were decreased but *Fos* protein levels were not changed at the time of analysis. In our SREBP2 knockdown experiments, gene expression analysis was performed 36 h after siRNA transfection. Therefore, we might observe primary changes of gene expression induced by SREBP2 down-regulation. Moreover, the

Fig. 2. Fatostatin inhibited osteoclast differentiation *in vitro*. A) Mature SREBP2 protein levels from osteoclasts treated with or without RANKL/fatostatin were measured by Western blotting. RAW264 cells were treated with vehicle or fatostatin (10 μM) with or without RANKL for 24 h. Actin was used as a loading control. Right panel shows quantification of normalized mature SREBP2 levels to actin controls. B) The number of TRAP-positive multinucleated cells (TRAP + MNCs) was counted (n = 4 biological replicates). Bars represent means ± SD. **, $p < 0.01$ versus vehicle control. Left panels show representative images of TRAP staining of osteoclasts treated with vehicle or fatostatin. C–E) Relative mRNA expression levels of osteoclast marker genes treated with vehicle or fatostatin for C) 24 h, D) 48 h and E) 72 h were measured by RT-qPCR (n = 3 biological replicates). Bars represent means ± SD.

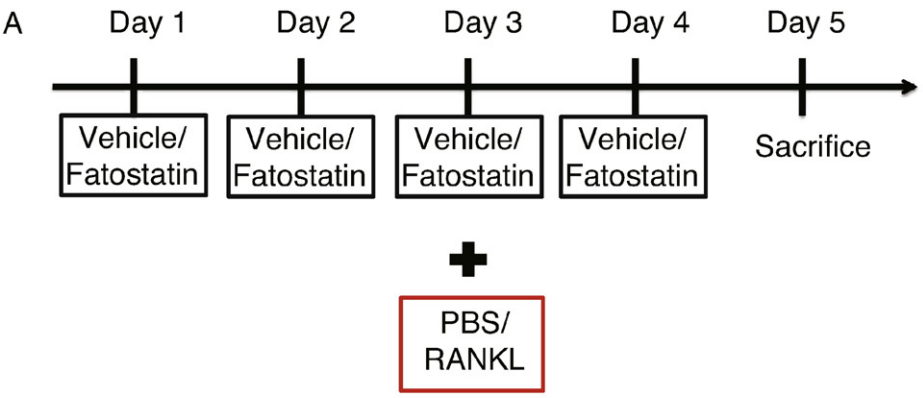
A
Day 1
Day 2
Day 3
Day 4
Day 5
Vehicle/ Fatostatin
Vehicle/ Fatostatin
Vehicle/ Fatostatin
Vehicle/ Fatostatin
Sacrifice
PBS/ RANKL

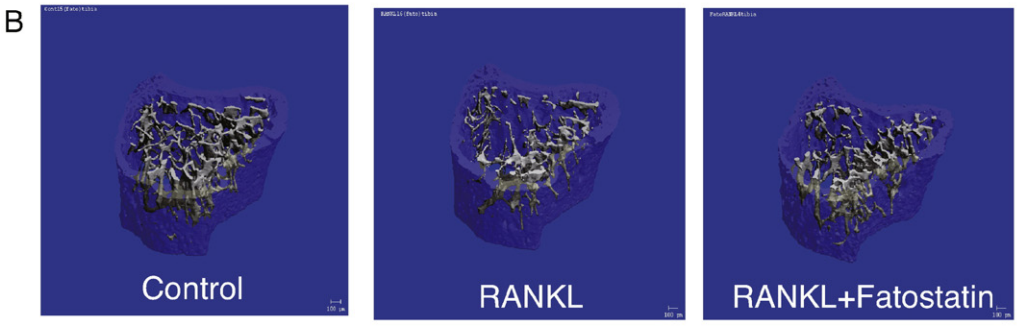
B
Control
RANKL
RANKL+Fatostatin

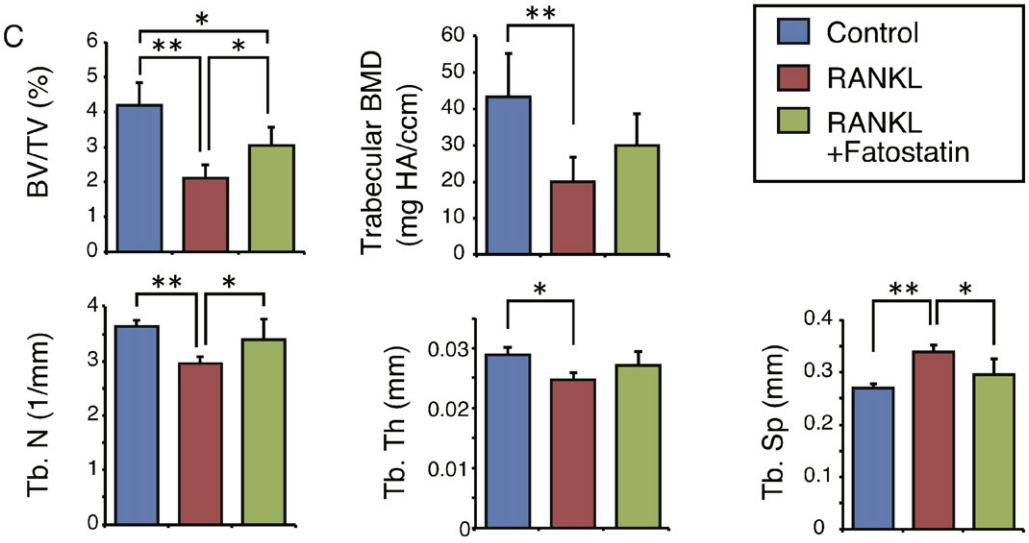
C
BV/TV (%)
Trabecular BMD (mg HA/ccm)
Control
RANKL
RANKL +Fatostatin
Tb. N (1/mm)
Tb. Th (mm)
Tb. Sp (mm)

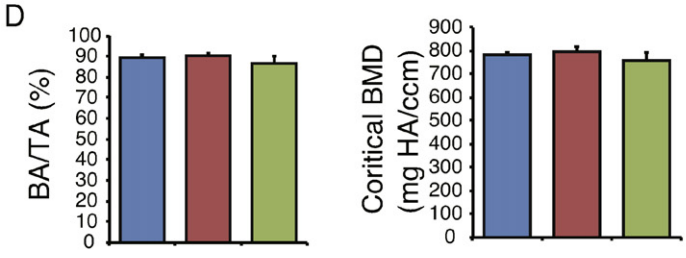
D
BA/TA (%)
Coritical BMD (mg HA/ccm)

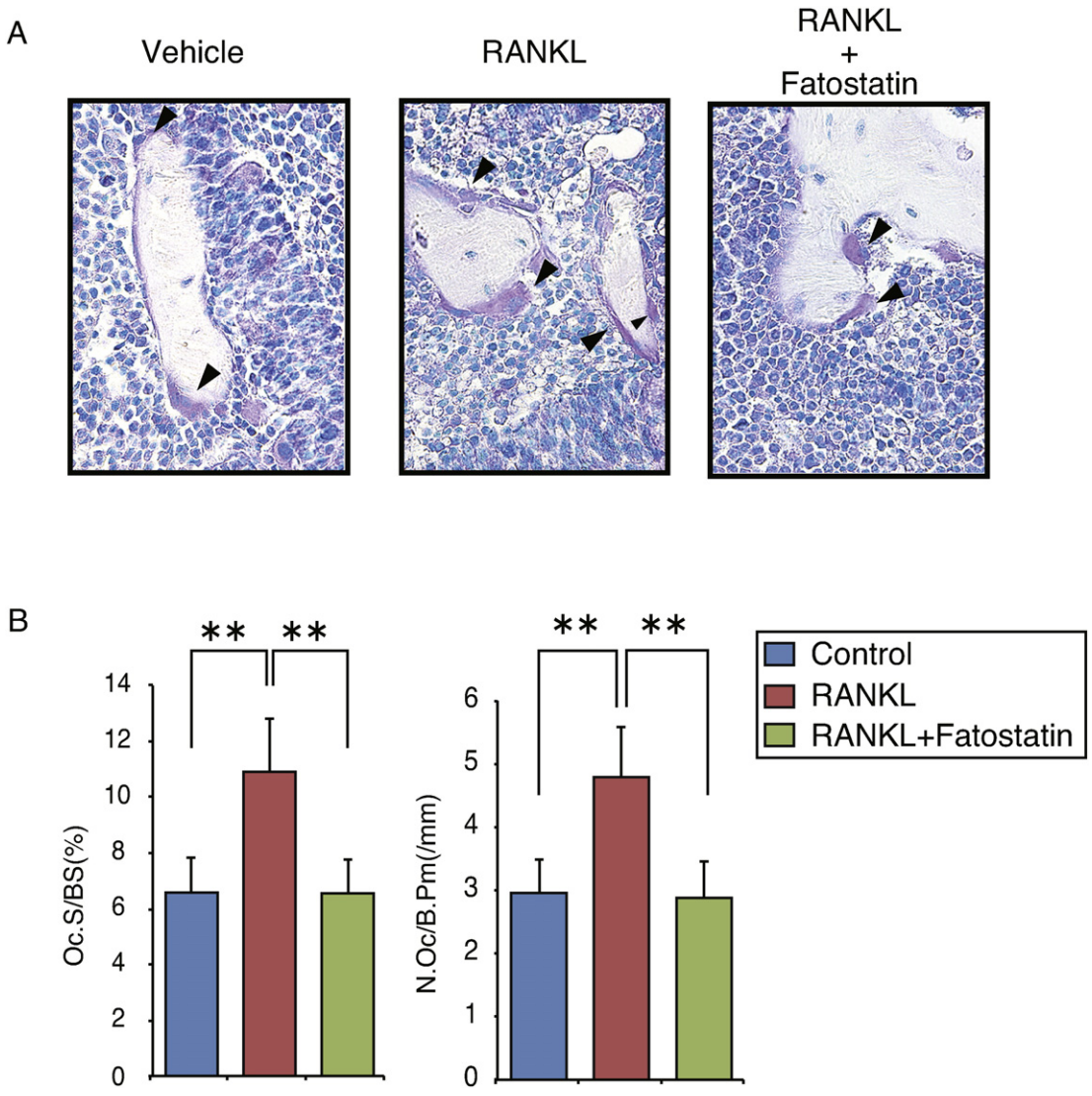

Fig. 4. Fatostatin suppressed osteoclast differentiation in the RANKL-induced bone loss model. A) Representative images of TRAP staining of proximal tibial metaphyses in mice treated with PBS, or GST-RANKL plus vehicle or GST-RANKL plus fatostatin. B) Bone histomorphometric analysis of proximal tibial metaphyses in mice of each group. Bars represent means ± SD. n = 5/group, **, $p < 0.01$.

differences in the results of gene expression analyses from SREBP2 knockdown and fatostatin treatment might have been due to the differences in the time point of RNA isolation. To clarify the transcriptional networks regulated by SREBP2 in osteoclasts, identification of the target genes of SREBP2 by genome-wide analyses might be needed. A recent study succeeded in identifying SREBP2 target genes in mouse liver with ChIP-seq analysis [40]. Hence, we might be able to identify SREBP2 target genes in osteoclasts using ChIP-seq in combination with RNA-seq during osteoclast differentiation. This approach might provide novel insights into transcriptional regulatory mechanisms underlying osteoclast differentiation and functions.

In addition, we demonstrated that inhibition of SREBP2 activation with fatostatin suppressed osteoclast differentiation both *in vivo* and *in vitro* and maintained bone mass in a RANKL-induced bone loss model. These results suggested that SREBP2 might be a positive regulator of osteoclast differentiation and inhibitors of SREBP2 activation may offer potential therapeutic treatments for osteoporosis or bone destruction in rheumatoid arthritis. In the RANKL-induced bone loss model, we used fatostatin for short periods. Long-term treatment with fatostatin reportedly led to reduced body weight and improved blood glucose and hepatic fat accumulation in *Ob/Ob* mice [30]. However, our results showed that long-term treatment with fatostatin under physiological conditions did not affect bone or cholesterol metabolism, suggesting that fatostatin might be effective for bone and lipid metabolism under pathological conditions. Whereas fatostatin treatment did not affect cortical bone metabolism in our model (Fig. 3D), *Srebf1* mRNA was increased during osteoblast differentiation (Fig. 1A). This result suggested that fatostatin might affect osteoblast differentiation. The RANKL-induced bone loss model, which lasts for just two days, is convenient for rapid analysis of osteoclast differentiation *in vivo*. However, this model may not be appropriate for evaluation of the effects of fatostatin on osteoblast differentiation because bone histomorphometric analyses

Fig. 3. Fatostatin suppressed bone loss in a RANKL-induced bone loss model. A) Schematic representation of the experimental schedule for the RANKL-induced bone loss model treated with vehicle or fatostatin. B) Representative reconstructed 3D μCT images of proximal tibia in mice treated with PBS (control), GST-RANKL plus vehicle (RANKL) or GST-RANKL along with fatostatin (RANKL + fatostatin). C) Quantitative μCT analysis of trabecular structure in mice of each group. D) Quantitative μCT analysis of cortical structure in mice of each group. Bars represent means ± SD. n = 5/group, *, $p < 0.05$ and **, $p < 0.01$.

revealed osteoblastic bone formation parameters were not changed [31] and osteoblast differentiation processes need a longer period for assessment. Therefore, it would be preferable to evaluate the effects of long-term administration of fatostatin on bone and/or other tissues using an ovariectomized mouse bone loss model.

Fatostatin was originally discovered as an adipogenesis-blocking reagent [41]. However, fatostatin also has anti-tumor activity that impaired the proliferation of IGF-associated tumors, including hepatocellular carcinoma (Hep-G2 cells) and prostate cancer (DU145 cells) [41]. In our study, fatostatin reduced TRAP-positive multinucleated osteoclasts and suppressed the expression of osteoclast genes, including *Fos*, *Nfatc1*, *CtsK* and *Acp5*. These results suggested that fatostatin might inhibit osteoclast differentiation, but it is also possible that fatostatin may inhibit proliferation of osteoclast precursors.

Inhibition of SREBP2 activation with fatostatin revealed pathophysiological functions of SREBP2 in osteoclast differentiation and bone metabolism. However, we cannot rule out indirect effects of fatostatin on bone metabolism mediated through other tissues or other types of cells. Therefore, genetic mouse models lacking *Srebf2*/SREBP2 should be examined to reveal the physiological functions of SREBP2 in osteoclasts. Because of the embryonic lethality in systemic SREBP2 null mice, osteoclast specific SREBP2-deficient mice should be generated using Cre/loxP technology. SREBP2 floxed mice have not yet been reported, but International Knockout Mouse Consortium groups are generating a conditional knockout resource [42]. Such a strain would be very useful for the generation of conditional SREBP2-deficient mice, permitting the clarification of the exact physiological functions of SREBP2. Towards that end, it is likely that macrophage/monocyte-specific LyzM-Cre mice [43] or CD11b-Cre [44] or osteoclast progenitor specific RANK-Cre mice [45] would be applicable. Analysis of bone phenotypes in macrophage/osteoclast-specific SREBP2-deficient mice will clarify the molecular basis of SREBP2 in osteoclast differentiation and will provide novel insights into osteoclast biology.

In conclusion, our study demonstrated that SREBP2 might be a novel transcription factor regulating osteoclast differentiation both *in vivo* and *in vitro*. In addition, this study revealed that transcription factors regulating cell differentiation that are identified by integrative genome-wide analyses (such as DNase-seq) have physiological functions and might offer therapeutic targets. Even though further studies are needed to elucidate the precise molecular basis of SREBP2 functions in bone metabolism, SREBP2-specific inhibitors might provide novel therapeutic strategies for osteoporosis.

Supplementary data to this article can be found online at http://dx.doi.org/10.1016/j.bbadis.2015.08.018.

Acknowledgment

The authors thank Dr. Tadahiro Iimura and Dr. Min-Young Youn for their technical advice, Mr. Rinya Masuko for his advice on μCT analysis, and the members of the Division of Laboratory Animal Research and the Division of Analytical Bio-Medicine, Advanced Research Support Center, Ehime University, for their technical assistance and helpful support.

This study was supported in part by JSPS KAKENHI Grant No. 23689066 and 15H04961 to YI, Scientific research grant from The Naito Foundation to YI, and Ehime University Internal Grants to YI and KI.

References

[1] T.J. Martin, N.A. Sims, Osteoclast-derived activity in the coupling of bone formation to resorption, Trends Mol. Med. 11 (2005) 76–81, http://dx.doi.org/10.1016/j.molmed.2004.12.004.
[2] N.A. Sims, T.J. Martin, Coupling the activities of bone formation and resorption: a multitude of signals within the basic multicellular unit, Bonekey Rep 3 (2014) 481, http://dx.doi.org/10.1038/bonekey.2013.215.
[3] S.L. Teitelbaum, Bone resorption by osteoclasts, Science 289 (2000) 1504–1508.
[4] S.L. Teitelbaum, F.P. Ross, Genetic regulation of osteoclast development and function, Nat. Rev. Genet. 4 (2003) 638–649, http://dx.doi.org/10.1038/nrg1122.
[5] A.E. Grigoriadis, Z.Q. Wang, M.G. Cecchini, W. Hofstetter, R. Felix, H.A. Fleisch, E.F. Wagner, c-Fos: a key regulator of osteoclast-macrophage lineage determination and bone remodeling, Science 266 (1994) 443–448.
[6] H. Takayanagi, S. Kim, T. Koga, H. Nishina, M. Isshiki, H. Yoshida, A. Saiura, M. Isobe, T. Yokochi, J. Inoue, E.F. Wagner, T.W. Mak, T. Kodama, T. Taniguchi, Induction and activation of the transcription factor NFATc1 (NFAT2) integrate RANKL signaling in terminal differentiation of osteoclasts, Dev. Cell 3 (2002) 889–901.
[7] C.P. Price, A. Kirwan, C. Vader, Tartrate-resistant acid phosphatase as a marker of bone resorption, Clin. Chem. 41 (1995) 641–643.
[8] F.H. Drake, R.A. Dodds, I.E. James, J.R. Connor, C. Debouck, S. Richardson, E. Lee-Rykaczewski, L. Coleman, D. Rieman, R. Barthlow, G. Hastings, M. Gowen, Cathepsin K, but not cathepsins B, L, or S, is abundantly expressed in human osteoclasts, J. Biol. Chem. 271 (1996) 12511–12516.
[9] K. Inoue, Y. Imai, Identification of novel transcription factors in osteoclast differentiation using genome-wide analysis of open chromatin determined by DNase-seq, J. Bone Miner. Res. 29 (2014) 1823–1832, http://dx.doi.org/10.1002/jbmr.2229.
[10] H.H. He, C.A. Meyer, M.W. Chen, V.C. Jordan, M. Brown, X.S. Liu, Differential DNase I hypersensitivity reveals factor-dependent chromatin dynamics, Genome Res. 22 (2012) 1015–1025, http://dx.doi.org/10.1101/gr.133280.111.
[11] H. Shimano, SREBPs: physiology and pathophysiology of the SREBP family, FEBS J. 276 (2009) 616–621, http://dx.doi.org/10.1111/j.1742-4658.2008.06806.x.
[12] N. Hada, M. Okayasu, J. Ito, M. Nakayachi, C. Hayashida, T. Kaneda, N. Uchida, T. Muramatsu, C. Koike, M. Masuhara, T. Sato, Y. Hakeda, Receptor activator of NF-kappaB ligand-dependent expression of caveolin-1 in osteoclast precursors, and high dependency of osteoclastogenesis on exogenous lipoprotein, Bone 50 (2012) 226–236.
[13] E. Luegmayr, H. Glantschnig, G.A. Wesolowski, M.A. Gentile, J.E. Fisher, G.A. Rodan, A.A. Reszka, Osteoclast formation, survival and morphology are highly dependent on exogenous cholesterol/lipoproteins, Cell Death Differ. 11 (2004) S108–S118, http://dx.doi.org/10.1038/sj.cdd.4401399 (Suppl.).
[14] T. Sato, I. Morita, S. Murota, Involvement of cholesterol in osteoclast-like cell formation via cellular fusion, Bone 23 (1998) 135–140.
[15] M.R. Briggs, C. Yokoyama, X. Wang, M.S. Brown, J.L. Goldstein, Nuclear protein that binds sterol regulatory element of low density lipoprotein receptor promoter. I. Identification of the protein and delineation of its target nucleotide sequence, J. Biol. Chem. 268 (1993) 14490–14496.
[16] S.M. Vallett, H.B. Sanchez, J.M. Rosenfeld, T.F. Osborne, A direct role for sterol regulatory element binding protein in activation of 3-hydroxy-3-methylglutaryl coenzyme A reductase gene, J. Biol. Chem. 271 (1996) 12247–12253.
[17] X. Hua, C. Yokoyama, J. Wu, M.R. Briggs, M.S. Brown, J.L. Goldstein, X. Wang, SREBP-2, a second basic-helix-loop-helix-leucine zipper protein that stimulates transcription by binding to a sterol regulatory element, Proc. Natl. Acad. Sci. U. S. A. 90 (1993) 11603–11607.
[18] R.B. Rawson, R. DeBose-Boyd, J.L. Goldstein, M.S. Brown, Failure to cleave sterol regulatory element-binding proteins (SREBPs) causes cholesterol auxotrophy in Chinese hamster ovary cells with genetic absence of SREBP cleavage-activating protein, J. Biol. Chem. 274 (1999) 28549–28556.
[19] P.J. Espenshade, D. Cheng, J.L. Goldstein, M.S. Brown, Autocatalytic processing of site-1 protease removes propeptide and permits cleavage of sterol regulatory element-binding proteins, J. Biol. Chem. 274 (1999) 22795–22804.
[20] R.B. Rawson, N.G. Zelenski, D. Nijhawan, J. Ye, J. Sakai, M.T. Hasan, T.Y. Chang, M.S. Brown, J.L. Goldstein, Complementation cloning of S2P, a gene encoding a putative metalloprotease required for intramembrane cleavage of SREBPs, Mol. Cell 1 (1997) 47–57.
[21] J.R. Smith, T.F. Osborne, J.L. Goldstein, M.S. Brown, Identification of nucleotides responsible for enhancer activity of sterol regulatory element in low density lipoprotein receptor gene, J. Biol. Chem. 265 (1990) 2306–2310.
[22] J.D. Horton, I. Shimomura, M.S. Brown, R.E. Hammer, J.L. Goldstein, H. Shimano, Activation of cholesterol synthesis in preference to fatty acid synthesis in liver and adipose tissue of transgenic mice overproducing sterol regulatory element-binding protein-2, J. Clin. Invest. 101 (1998) 2331–2339, http://dx.doi.org/10.1172/JCI2961.
[23] L. Zeng, H. Liao, Y. Liu, T.S. Lee, M. Zhu, X. Wang, M.B. Stemerman, Y. Zhu, J.Y. Shyy, Sterol-responsive element-binding protein (SREBP) 2 down-regulates ATP-binding cassette transporter A1 in vascular endothelial cells: a novel role of SREBP in regulating cholesterol metabolism, J. Biol. Chem. 279 (2004) 48801–48807, http://dx.doi.org/10.1074/jbc.M407817200.
[24] K.L. Ma, J. Liu, C.X. Wang, J. Ni, Y. Zhang, Y. Wu, L.L. Lv, X.Z. Ruan, B.C. Liu, Activation of mTOR modulates SREBP-2 to induce foam cell formation through increased retinoblastoma protein phosphorylation, Cardiovasc. Res. 100 (2013) 450–460, http://dx.doi.org/10.1093/cvr/cvt203.
[25] K. Fon Tacer, S. Kalanj-Bognar, M.R. Waterman, D. Rozman, Lanosterol metabolism and sterol regulatory element binding protein (SREBP) expression in male germ cell maturation, J. Steroid Biochem. Mol. Biol. 85 (2003) 429–438.
[26] M. Ishikawa, Y. Iwasaki, S. Yatoh, T. Kato, S. Kumadaki, N. Inoue, T. Yamamoto, T. Matsuzaka, Y. Nakagawa, N. Yahagi, K. Kobayashi, A. Takahashi, N. Yamada, H. Shimano, Cholesterol accumulation and diabetes in pancreatic beta-cell-specific SREBP-2 transgenic mice: a new model for lipotoxicity, J. Lipid Res. 49 (2008) 2524–2534, http://dx.doi.org/10.1194/jlr.M800238-JLR200.
[27] K. Ma, P. Malhotra, V. Soni, O. Hedroug, F. Annaba, A. Dudeja, L. Shen, J.R. Turner, E.A. Khramtsova, S. Saksena, P.K. Dudeja, R.K. Gill, W.A. Alrefai, Overactivation of intestinal SREBP2 in mice increases serum cholesterol, PLoS One 9 (2014) e84221, http://dx.doi.org/10.1371/journal.pone.0084221.
[28] H. Shimano, Sterol regulatory element-binding proteins (SREBPs): transcriptional regulators of lipid synthetic genes, Prog. Lipid Res. 40 (2001) 439–452.

[29] H. Shimano, I. Shimomura, R.E. Hammer, J. Herz, J.L. Goldstein, M.S. Brown, J.D. Horton, Elevated levels of SREBP-2 and cholesterol synthesis in livers of mice homozygous for a targeted disruption of the SREBP-1 gene, J. Clin. Invest. 100 (1997) 2115–2124, http://dx.doi.org/10.1172/JCI119746.
[30] S. Kamisuki, Q. Mao, L. Abu-Elheiga, Z. Gu, A. Kugimiya, Y. Kwon, T. Shinohara, Y. Kawazoe, S. Sato, K. Asakura, H.Y. Choo, J. Sakai, S.J. Wakil, M. Uesugi, A small molecule that blocks fat synthesis by inhibiting the activation of SREBP, Chem. Biol. 16 (2009) 882–892, http://dx.doi.org/10.1016/j.chembiol.2009.07.007.
[31] Y. Tomimori, K. Mori, M. Koide, Y. Nakamichi, T. Ninomiya, N. Udagawa, H. Yasuda, Evaluation of pharmaceuticals with a novel 50-hour animal model of bone loss, J. Bone Miner. Res. 24 (2009) 1194–1205, http://dx.doi.org/10.1359/jbmr.090217.
[32] Y. Nakashima, T. Haneji, Stimulation of osteoclast formation by RANKL requires interferon regulatory factor-4 and is inhibited by simvastatin in a mouse model of bone loss, PLoS One 8 (2013) e72033, http://dx.doi.org/10.1371/journal.pone.0072033.
[33] S. Kondoh, K. Inoue, K. Igarashi, H. Sugizaki, Y. Shirode-Fukuda, E. Inoue, T. Yu, J.K. Takeuchi, J. Kanno, L.F. Bonewald, Y. Imai, Estrogen receptor alpha in osteocytes regulates trabecular bone formation in female mice, Bone 60 (2014) 68–77, http://dx.doi.org/10.1016/j.bone.2013.12.005.
[34] Y. Yamamoto, T. Yoshizawa, T. Fukuda, Y. Shirode-Fukuda, T. Yu, K. Sekine, T. Sato, H. Kawano, K. Aihara, Y. Nakamichi, T. Watanabe, M. Shindo, K. Inoue, E. Inoue, N. Tsuji, M. Hoshino, G. Karsenty, D. Metzger, P. Chambon, S. Kato, Y. Imai, Vitamin D receptor in osteoblasts is a negative regulator of bone mass control, Endocrinology 154 (2013) 1008–1020, http://dx.doi.org/10.1210/en.2012-1542.
[35] M.L. Bouxsein, S.K. Boyd, B.A. Christiansen, R.E. Guldberg, K.J. Jepsen, R. Muller, Guidelines for assessment of bone microstructure in rodents using micro-computed tomography, J. Bone Miner. Res. 25 (2010) 1468–1486, http://dx.doi.org/10.1002/jbmr.141.
[36] D.W. Dempster, J.E. Compston, M.K. Drezner, F.H. Glorieux, J.A. Kanis, H. Malluche, P.J. Meunier, S.M. Ott, R.R. Recker, A.M. Parfitt, Standardized nomenclature, symbols, and units for bone histomorphometry: a 2012 update of the report of the ASBMR Histomorphometry Nomenclature Committee, J. Bone Miner. Res. 28 (2013) 2–17, http://dx.doi.org/10.1002/jbmr.1805.
[37] M.Y. Youn, A. Yokoyama, S. Fujiyama-Nakamura, F. Ohtake, K. Minehata, H. Yasuda, T. Suzuki, S. Kato, Y. Imai, JMJD5, a Jumonji C (JmjC) domain-containing protein, negatively regulates osteoclastogenesis by facilitating NFATc1 protein degradation, J. Biol. Chem. 287 (2012) 12994–13004, http://dx.doi.org/10.1074/jbc.M111.323105.
[38] L. Danks, H. Takayanagi, Immunology and bone, J. Biochem. 154 (2013) 29–39, http://dx.doi.org/10.1093/jb/mvt049.
[39] M. Okayasu, M. Nakayachi, C. Hayashida, J. Ito, T. Kaneda, M. Masuhara, N. Suda, T. Sato, Y. Hakeda, Low-density lipoprotein receptor deficiency causes impaired osteoclastogenesis and increased bone mass in mice because of defect in osteoclastic cell–cell fusion, J. Biol. Chem. 287 (2012) 19229–19241, http://dx.doi.org/10.1074/jbc.M111.323600.
[40] Y.K. Seo, T.I. Jeon, H.K. Chong, J. Biesinger, X. Xie, T.F. Osborne, Genome-wide localization of SREBP-2 in hepatic chromatin predicts a role in autophagy, Cell Metab. 13 (2011) 367–375, http://dx.doi.org/10.1016/j.cmet.2011.03.005.
[41] Y. Choi, Y. Kawazoe, K. Murakami, H. Misawa, M. Uesugi, Identification of bioactive molecules by adipogenesis profiling of organic compounds, J. Biol. Chem. 278 (2003) 7320–7324, http://dx.doi.org/10.1074/jbc.M210283200.
[42] W.C. Skarnes, B. Rosen, A.P. West, M. Koutsourakis, W. Bushell, V. Iyer, A.O. Mujica, W. Bushell, V. Iyer, A.O. Mujica, M. Thomas, J. Harrow, T. Cox, D. Jackson, J. Severin, P. Biggs, J. Fu, M. Nefedov, P.J. de Jong, A.F. Stewart, A. Bradley, A conditional knockout resource for the genome-wide study of mouse gene function, Nature 474 (2011) 337–342, http://dx.doi.org/10.1038/nature10163.
[43] B.E. Clausen, C. Burkhardt, W. Reith, R. Renkawitz, I. Forster, Conditional gene targeting in macrophages and granulocytes using LysMcre mice, Transgenic Res. 8 (1999) 265–277.
[44] M. Ferron, J. Vacher, Targeted expression of Cre recombinase in macrophages and osteoclasts in transgenic mice, Genesis 41 (2005) 138–145, http://dx.doi.org/10.1002/gene.20108.
[45] K. Maeda, Y. Kobayashi, N. Udagawa, S. Uehara, A. Ishihara, T. Mizoguchi, Y. Kikuchi, I. Takada, S. Kato, S. Kani, M. Nishita, K. Marumo, T.J. Martin, Y. Minami, N. Takahashi, Wnt5a-Ror2 signaling between osteoblast-lineage cells and osteoclast precursors enhances osteoclastogenesis, Nat. Med. 18 (2012) 405–412, http://dx.doi.org/10.1038/nm.2653.